The official journal of the Japan Atherosclerosis Society and
the Asian Pacific Society of Atherosclerosis and Vascular Diseases

Original Article

J Atheroscler Thromb, 2021; 28: 716-729. http://doi.org/10.5551/jat.55343

Phenotypic Switching of Atherosclerotic Smooth Muscle Cells is Regulated by Activated PARP1-Dependent TET1 Expression

Chao Zhang[1], Xin Chen[1], Ju-Kun Wang[1], Yu Li[2], Shi-Jun Cui[2], Zhonggao Wang[1, 2] and Tao Luo[1]

Chao Zhang and Xin Chen contributed equally to this work.
Zhonggao Wang and Tao Luo are joint senior authors.

[1]Department of General Surgery, Xuanwu Hospital, Capital Medical University, Beijing, China
[2]Department of Vascular Surgery, Xuanwu Hospital, Capital Medical University, Beijing, China

Aim: During the development of atherosclerosis, the vascular smooth muscle cells (SMCs) undergo phenotypic switching from contractile phenotype to synthetic phenotype. This study aimed at examining the role of DNA modification mediated by the oxidative stress dependent ten eleven translocation enzymes (TETs) expression at early stage of phenotypic switching.

Methods: Based on the *in vitro* SMCs calcification model, DNA damage, phenotypic switching and 5-hydroxymethylcytosine (5hmC) were examined by comet assay, alkaline DNA unwinding assay, immunofluorescence staining, Dot blotting and Western blotting. Then Western blotting and qRT-PCR were performed to analyze the TETs expression and the relationship between the activity of poly(ADP-ribose) polymerase 1 (PARP1) and TETs expression. We further alter 5hmC modification by inhibition of TET1 or PARP1 to rescue the phenotypic switching of SMCs using immunofluorescence staining, Dot blotting and qRT-PCR. We performed immunochemistry staining to examine the activated PARP1-TET1 pathway *in vivo*.

Results: The phenotypic switching was observed in the SMCs cultured with calcification medium as the expression of the cell markers of contractile SMCs decreased and cell proliferation increased. In contrast, PAR and 5hmC were markedly increased in SMCs with calcification due to DNA damage. Our study further demonstrated that oxidative stress-activated PARP1, promotes TET1 expression and 5hmC increase during the phenotypic switching. Inhibition of TET1 or PARP1 can rescue the phenotypic switching of SMCs with calcification.

Conclusion: Our study demonstrated the important role of PARylation dependent 5hmC, in SMCs phenotypic switching. It raises the possibility to target TET1 and PARP1 for atherosclerosis treatment.

Key words: Atherosclerosis, Phenotypic switching, Poly (ADP-ribose) polymerase 1, Ten–eleven translocation enzyme 1, Vascular smooth muscle cells

Introduction

Atherosclerosis is a chronic vascular disease characterized by the formation of lipid-rich plaque within the arterial wall[1, 2]. Vascular smooth muscle cells (SMCs) are the major cell type in atherosclerotic plaques[3]. During the development of atherosclerosis, the SMCs may shift from a quiescent, contractile phenotype to a synthetic phenotype, which is called phenotypic switching[4]. Phenotypic switching plays a critical role in the process of atherosclerosis[4]. However, the molecular mechanisms under phenotypic switching are still unclear. During phenotypic switching, the gene expression profile of SMCs changes dramatically[4, 5]. It is widely believed that epigenetic modifications are the key processes in cell differentiation and control cell-specific marker[6]. Furthermore, accumulated studies have demonstrated the role of epigenetic

Address for correspondence: Tao Luo, Department of General Surgery, Xuanwu Hospital of Capital Medical University, Beijing, 100053, China
E-mail: Taoluo35@126.com

Received: January 21, 2021 Accepted for publication: July 21, 2020

changes in vascular atherosclerosis, including DNA and histone modification[7]. It has been reported that DNA methylation might participate in regulating SMCs phenotype and vascular remodeling[8, 9]. To explore the possibility of epigenetic modification as therapeutic target for atherosclerosis treatment, we further analyzed the upstream factors regulating epigenetic modification at early stage of phenotypic switching. By establishing *in vitro* SMCs calcification model, we found that oxidative stress in the SMCs during calcification induction can activate poly(ADP-ribose) polymerase 1 (PARP1) and further promote ten–eleven translocation enzyme 1 (TET1) expression. Global increase of 5-hydroxymethylcytosine (5hmC) level caused by elevated TET1 level will regulate the phenotypic switching in SMCs. Therefore, the present study suggested that PARP1 and TET1 would act as the potential target for atherosclerosis treatment.

Materials and Methods

Antibodies

Rabbit anti-5hmC polyclonal antibody (#39769) was purchased from Active Motif (Carlsbad, CA, USA). Mouse anti-β-actin monoclonal antibody (AC-15) (#A1978) was purchased from Sigma (St. Louis, MO, USA). Mouse anti-PAR monoclonal antibody (#4335-MC-100) was purchased from Trevigen (Gaithersburg, MD, USA). Rabbit anti-α-SMA polyclonal antibody (#ab5694) was purchased from Abcam (Cambridge, UK). Rabbit anti-TET1 polyclonal antibody (#ABE1034) was purchased from Millipore (Burlington, MA, USA). Rabbit anti-Ki67 polyclonal antibody (#15580) was purchased from Abcam (Cambridge, UK).

SMC Culture and Induction of Calcification

Mouse aortic SMCs (MOVAS, CRL-2797™, ATCC) were cultured in Dulbecco's Modified Eagle Media (DMEM) supplemented with 10% bovine serum and 100 U/ml penicillin, and 100 mg/ml streptomycin. For induction of calcification, MOVAS were seeded in culture dishes at a density of 1.5×10^5 cells/cm^2 and maintained in 10% fetal bovine serum–DMEM (high glucose). After they become 70%–80% confluent, NaH_2PO_4/Na_2HPO_4 and $CaCl_2$ were added to the culture medium to final concentration of 3.0 and 2.7 mM, respectively, for 7 days to induce calcification. The medium was replaced every 48 h.

Sample Collection

The carotid artery tissues were surgically removed from the patients with carotid restenosis following CAS treatment at the Xuanwu Hospital of Capital Medical University in China and were harvested for the present study according to informed consent principles.

Von Kossa Staining

The calcification of MOVAS was detected via von Kossa staining according to the standard protocol. The cultured MOVAS were washed with phosphate-buffered saline (PBS) twice and fixed with 4% paraformaldehyde for 1 h. Then, VSMCs were incubated with 2% silver nitrate solution under ultraviolet light for 20 min. After 4 rinses with distilled water, the cells were neutralized in 5% sodium thiosulfate for 5 min. Then, the cells were counterstained with 1% neutral red for 1 min and imaged using a digital camera.

Immunofluorescence and Immunochemistry Staining

MOVAS grown on coverslips were fixed with 4% paraformaldehyde for 20 min and permeabilized with 0.5% Triton X-100 in PBS for 5 min at room temperature. Then, cells were washed with cold PBS and incubated with blocking buffer (10% donkey serum, 3% bovine serum albumin in PBS containing 0.1% Triton X-100) before incubation with primary antibodies overnight in a humidified chamber at 4℃. For 5hmC staining, permeabilized cells were denatured with 2 N HCl for 30 min, neutralized with 100 mM Tris–HCl (pH 8.5) before blocking. After 3 consecutive 5 min washes with PBS, cells were incubated with Cy3-conjugated secondary antibodies for 30 min. Then, the cells were washed again three times with PBS and mounted onto glass slides and visualized by a fluorescence microscope. Intensity of immunofluorescence was measured by ImageJ.

The artery specimens were fixed in 4% paraformaldehyde for 24 h, dehydrated, embedded into paraffin wax, and then sectioned to 4 μm slides and processed for immunochemistry (IHC) staining. To conduct IHC staining, sections were deparaffinized and incubated with rabbit anti-TET1 (1:500), mouse anti-PAR (1:500), and rabbit anti-5hmC (1:500). Then, the slides were washed in PBS and incubated with horseradish peroxidase (HRP)-conjugated secondary antibodies (1:1000, Jackson ImmunoResearch Laboratories) at room temperature for 30 min. After washing with PBS three times, 3,3'-diaminobenzidine (DAB) substrate solution was applied to the sections on the slides to reveal the color of antibody staining. Then, the slides were washed in PBS and counterstained with hematoxylin for 1–2 min. After rinsing with running water for 15 min, the slides were covered with coverslips. The color of antibody staining in the tissue section was observed under microscopy.

Table 1. List of qPCR primers

Genes		Sequence (5'-3')
MYH11	Forward	AACTGGCAATGGTGGCGGCTCTTC
	Reverse	TCAGCATACAGCTCTGTCTCTGCC
SM22α	Forward	AGTGGAGTGGATTGTAGTGCAGTG
	Reverse	TCTTGATGACTCCATAATCTTCAGC
SRF	Forward	TGAAGATCAAGATGGAGTTCATCG
	Reverse	CGAGTTGAGGCAGGTCTGAATCAGC
MYOCD	Forward	ATTCTGCCGATGGATTCTTCCGTG
	Reverse	ATCATTCTTGTCACTTTCTGAGCC
ICAM1	Forward	TTCCGCTACCATCACCGTGTATTCG
	Reverse	AGCCAGCACCGTGAATGTGATCTCC
CK8	Forward	TTGCAGCAGCAGAAGACGTCGAGG
	Reverse	TTCATGTATGCTTCGTCCACATCC
KLF4	Forward	AGCTGGTGCAGCTTGCAGCAGTAAC
	Reverse	TCGGATAGCTGAAGCTGCAGGTGG
LGALS3	Forward	TACCCAGGACAGGCTCCTCCTAGTG
	Reverse	AGCAGGATAGCCTCCAGGAGCACTG
GAPDH	Forward	CATCACTGCCACCCAGAAGACTG
	Reverse	ATGCCAGTGAGCTTCCCGTTCAG
TET1	Forward	GAGCCTGTTCCTCGATGTGG
	Reverse	CAAACCCACCTGAGGCTGTT
TET2	Forward	AACCTGGCTACTGTCATTGCTCCA
	Reverse	ATGTTCTGCTGGTCTCTGTGGGAA
TET3	Forward	GTCTCCCCAGTCCTACCTCCG
	Reverse	GTCAGTGCCCCACGCTTCA

Dot Blotting Assay

Genomic DNA from MOVAS was denatured by 0.2 N NaOH and dotted on Hybond-N+ nitrocellulose membrane (Amersham Pharmacia Biotech). After drying at 65℃, the membrane was blocked with 10% non-fat milk for 1 h at room temperature followed by 2 h incubation with anti-5hmC antibodies at room temperature. After 3 consecutive 10 min washes with Tris-buffered saline with Tween®-20 (TBST), the membrane was incubated with HRP-conjugated goat-anti-rabbit secondary antibody for 1 h. The membrane was washed again three times with TBST and developed using the Enhanced ChemiLuminescence plus (ECL+) detection system (GE Healthcare).

Quantitative Real-Time Polymerase Chain Reaction

Quantitative real-time polymerase chain reaction (qRT-PCR). Total RNA was isolated from MOVAS using TRIzol reagent (Thermo Fisher Scientific) according to the manufacturer's protocol. RNA was reverse transcribed with High-Capacity Reverse Transcription Kit (Thermo Fisher Scientific) by using 1 μg RNA. Gene expression analysis was conducted by using SYBR Green Master Mix (Thermo Fisher Scientific) in Biorad real-time PCR instrument. The level of each mRNA was normalized to the level of the GAPDH mRNA in each sample. The comparative CT method ($2^{-\Delta\Delta CT}$) was used to calculate the average fold differences between pairs of samples. Each reaction was conducted in triplicate. The primers used for qRT-PCR are shown in **Table 1**.

Transfection of siRNAs to MOVAS

MOVAS were transfected TET1 siRNAs (siTET1) and Mock siRNAs (Mock) using Lipofectamine 2000 (Thermo Fisher Scientific) at final concentration of 100 nM. TET1 siRNAs and Mock siRNAs were designed and purchased from Dharmacon (Lafayette, CO, USA). The siRNA TET1 sense sequence is 5'-GCAGAUGGCCGUGACACAA-3', and the mock siRNA sense sequence is 5'-CUACAACUCCC ACAACGUA-3'.

PARP InhibitorTreatment

Olaparib was purchased from AdooQ Bioscience. MOVAS were treated with olaparib at final concentration of 5 μM during the induction of calcification. The cells were incubated with olaparib for 12 h each time before the fresh induction medium was replaced at days 0, 2, 4, and 6.

Protein Extraction and Western Blotting

Protein samples were extracted from MOVAS by using NETN300 lysis buffer (0.5% NP-40, 50 mM Tris–HCl pH 8.0, 2 mM ethylenediaminetetraacetic acid [EDTA], and 300 mM NaCl) containing 10 mM NaF and 50 mM β-glycerophosphate. The protein concentration was determined using BCA standard curve. Equal amounts of protein extracts were separated using sodium dodecyl sulfate polyacrylamide gel electrophoresis and transferred electrophoretically to polyvinylidene difluoride membranes (Millipore). The membranes were blocked in TBST containing 5% milk at room temperature for 1 h. After washing with TBST, the blocked membranes were probed with indicated primary antibodies overnight at 4℃. After 3 consecutive 10 min washes with TBST, the membranes were incubated with HRP-conjugated goat-anti-rabbit or goat-anti-mouse secondary antibody for 1 h. The membranes were washed again 3 times with TBST and developed using the ECL+ detection system (GE Healthcare).

Alkaline DNA Unwinding Assay

MOVAS were seeded in 24-well plates at a density of 5×10^4 cells per well. After 24 h, cells were labeled with 3H-TdR (7.1 kBq/ml) for an additional 24 h. Cells were lysed in the DNA unwinding solution (0.15 M NaCl, 30 mM NaOH) on ice for 30 min in darkness. Then, lysates were neutralized by the addition of 20 mM NaH2PO4 and fragmented by sonication (15 s, Branson sonifier B-12, with micro tip). Then, samples were added with 0.24% of sodium dodecyl sulfate and kept frozen at −20℃ for at least 12 h. Separation of double- and single-stranded DNA was conducted on hydroxyl apatite columns, kept at 60℃, as previously described[10]. Briefly, 1 ml of cell lysates was loaded on to the column and washed with 6 ml of sodium phosphate (10 mM). Single-stranded DNA was eluted with 4.25 ml potassium phosphate (0.1 M) and double-stranded DNA was eluted with 4.25 ml potassium phosphate at (0.25 M). The number of SSBs per cell was calculated from the ratio of single- DNA to double-stranded DNA by correlation with a standard curve.

Alkaline Comet Assay

MOVAS were collected and rinsed twice with ice cold PBS at indicated time points. 1×10^5 cells/ml were combined with LMAgarose at 37℃ at a ratio of 1:10 (v/v) and immediately pipetted onto slides. For cell lysis, the slides were immersed in the neutral lysis solution (1.2 M NaCl, 100 mM Na2EDTA, 0.1% sodium lauryl sarcosinate, 0.26 M NaOH (pH>13)) overnight at 4℃ in the dark. Then, the slides were subjected to electrophoresis (0.03 M NaOH, 2 mM Na2EDTA (pH ~ 12.3)) at 15 V for 25 min (0.6 V/cm), and stained in 10 μg/ml propidium iodide for 20 min. Images were taken with a fluorescence microscope and analyzed with the CometScore software.

Statistical Analysis

All the experiments were conducted at least three times. Two-tailed Student's *t* test was used for comparing the two groups. Data were presented as mean ± SD, $p<0.05$ were considered statistically significant.

Results

Calcification Induces Phenotypic Switching in MOVAS

To investigating the molecular mechanisms of phenotypic switching in MOVAS, we established the *in vitro* MOVAS calcification model according to the previous report[11]. Significant calcification was detected in MOVAS cultured with calcification medium for 7 days **(Fig. 1A)**. As expected, the bone markers, including CFBA1 and osteopontin (OPN), were highly induced by calcification medium containing high concentration of phosphate **(Fig. 1B)**. We further examined the change of SMCs marker in MOVAS with calcification medium culture. The expression of α-SMA, one of the frequently used markers of SMCs, was found to be significantly decreased after calcification of the MOVAS **(Fig. 1C–E)**.

Calcification Induces 5hmC Increase in MOVAS

Epigenetic modification plays a key role in regulating gene expression in various physiological and pathological processes. As one of the most important epigenetic modifications, DNA methylation has been reported to be involved in the phenotypic switching of SMCs during vascular atherosclerosis[12]. TET proteins are the major enzymes in active DNA demethylation by oxidizing 5-methylcytosine (5 mC)[13, 14]. 5hmC is the first oxidative product of TET proteins. Thus, we explored the potential role of 5hmC in phenotypic switching of SMCs. Interestingly, we found that 5hmC level was significantly increased in the MOVAS cultured with calcification medium compared with those with regular medium culture **(Fig. 2A–C)**. Since TET proteins, TET1, TET2, and TET3, are the only three enzymes converting 5 mC to 5hmC, we further examined the expression level of TET1, TET2, and TET3 under high concentration of phosphate. The expression of TET1, but not TET2 or TET3, was found to be enhanced by calcification medium in MOVAS **(Fig. 2D–E)**.

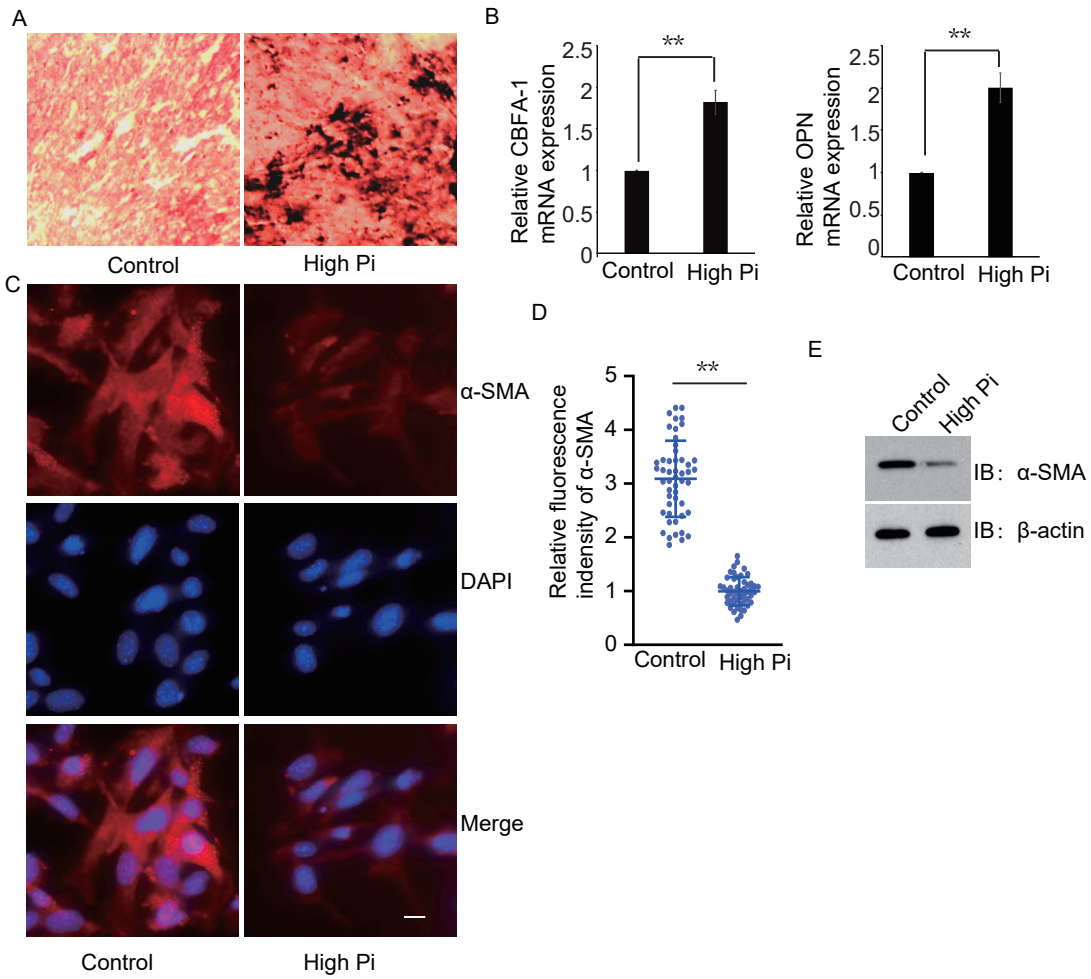

Fig. 1. High concentration of phosphate induces calcification and the phenotypic switching in MOVAS

(A) Von Kossa staining was conducted to detect the calcification. Significant calcification was observed in MOVAS cultured in the medium with high concentration of phosphate for 7 days. (B) The key genes associated with vascular calcification was examined using qPCR. Significant increase of CBFA-1 and OPN expression was shown in the MOVAS with calcification medium culture. Three independent experiments were conducted. Data are presented as mean ± SD, $^{**}p < 0.01$. Data were analyzed using two-tailed unpaired Student's *t* tests. (C) α-SMA expression was detected by immunofluorescence staining. Significant decrease of α-SMA expression was induced by high concentration of phosphate in MOVAS. Bar: 10 μm. (D) Quantification of α-SMA expression level in MOVAS was summarized from the immunostaining results. Scatter plots represent for α-SMA expression level in each cell. Fifty cells in each group were analyzed by ImageJ. $^{**}p < 0.01$. (E) Western blotting was conducted to confirm the decrease of α-SMA expression in MOVAS treated with high concentration of phosphate for 7 days.

Calcification Causes DNA Damage in MOVAS

We further asked the potential upstream factors that may be involved in the TET1-mediated 5hmC increase in MOVAS calcification. Accumulated evidences showed that DNA damage caused by oxidative stress occurred in the atherosclerotic vascular cells[15, 16]. Thus, we examined the DNA damage in MOVAS with calcification medium culture. Since oxidative stress can cause both DNA double-stranded breaks (DSBs) and single-stranded breaks (SSBs), we examined DSBs and SSBs [17, 18]. We found that high concentration of phosphate induced significant increase of γH2AX foci, a sensitive marker of DSBs **(Fig. 3A–B)**. SSBs were also detected by alkaline comet assay and alkaline DNA unwinding assay in MOVAS cultured with either regular medium or calcification medium[10, 19]. Consistent with the result of DSBs, SSBs were also significantly accumulated in the MOVAS cultured with calcification medium **(Fig. 3C–D)**. It has been well known that DNA breaks caused by oxidative stress can activate the DNA nick sensor enzyme PARP-1, the most potent part of the 17-member PARP enzyme family[20]. Emerging evidence has shown that PARP1 plays an important role in both DSBs and SSBs repair[21-24]. Using NAD+ as the ADP-ribose (ADPr) donor, activated PARP1

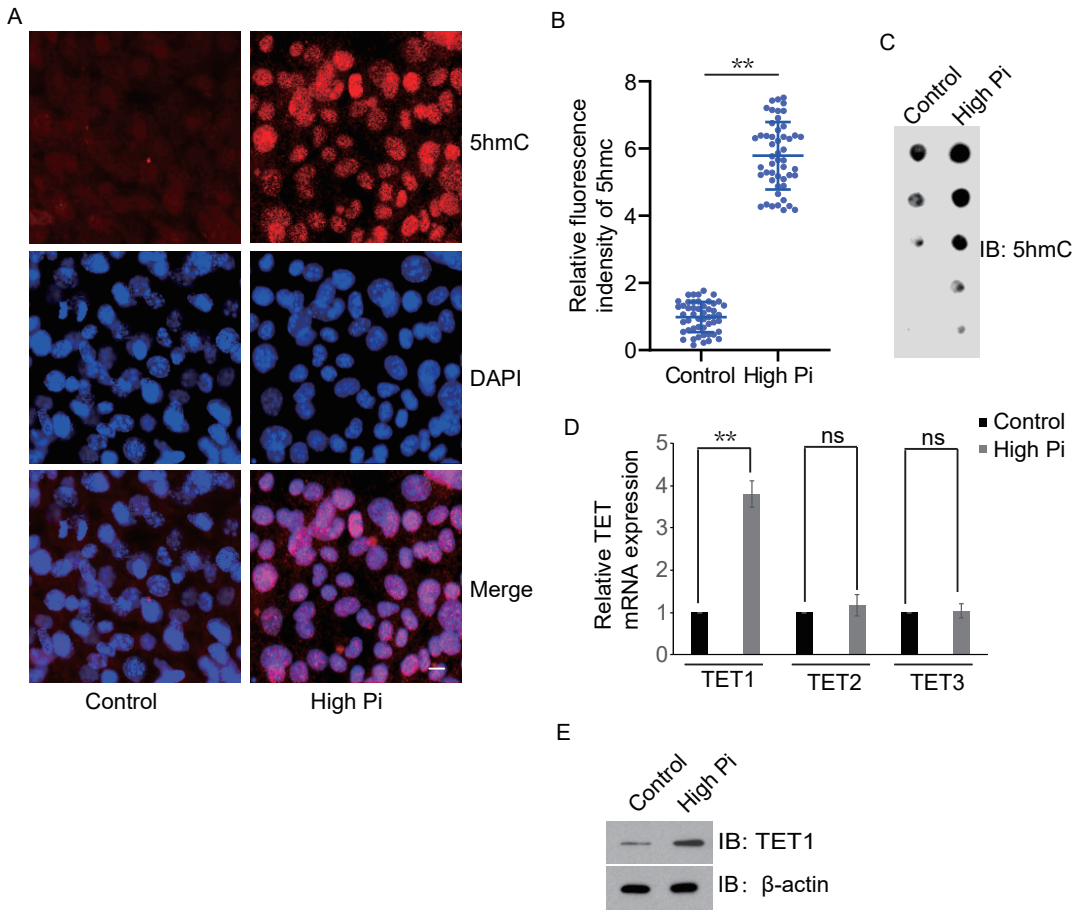

Fig. 2. High concentration of phosphate increases 5hmC level in MOVAS

(A) Immunostaining results showed the increase of 5hmC in MOVAS with calcification medium culture compared with those in control medium. Bar: 10 μm. (B) Quantification of 5hmC level in MOVAS was summarized from the immunostaining results. Fifty cells in each group were analyzed by ImageJ. $^{**}p<0.01$. (C) Dot blotting was conducted to further examine the 5hmC level in MOVAS. Compared with control cells, the cells cultured with high-phosphate medium showed significant increase of 5hmC level. (D) The mRNA expression of TET1, TET2, and TET3 was examined by qPCR. TET1, but not TET2 or TET3, was increased by high concentration of phosphate in MOVAS. Three independent experiments were conducted. Data are presented as mean ± SD, $^{**}p<0.01$, ns: not significant. Data were analyzed using two-tailed unpaired Student's *t* tests. (E) Western blotting was conducted to confirm the increase of TET1 protein level in MOVAS with calcification medium culture.

synthesizes both linear and branched polymer chains of ADPr, poly(ADP-ribose) (PAR)[25]. Hence, we examined the level of PAR in MOVAS with calcification medium culture. Compared with control MOVAS, the MOVAS with calcification medium culture showed higher level of PAR **(Fig. 3E)**.

Activated PARP1 Promotes TET1 Expression in MOVAS Calcification

To explore the causative relationship between PARP1 activation and TET1 expression, we treated MOVAS with olaparib, a PARP1 inhibitor, under calcification medium culture[26]. It is of interest that olaparib significantly decreased the TET1 expression induced by SMCs calcification **(Fig. 4A)**. Consistently, olaparib treatment reversed the induction of 5hmC by calcification medium in MOVAS **(Fig. 4B)**. We further transfected MOVAS with TET1 siRNAs to compare the effect of both TET1 knockdown and PARP inhibition on 5hmC level in MOVAS calcification **(Fig. 4C)**. The immunostaining results showed that either siTET1 or olaparib could decrease the 5hmC level to a similar extent in MOVAS treated with high concentration of phosphate **(Fig. 4D-E)**. Therefore, high expression of TET1 during MOVAS calcification was mediated by activated PARP1.

Inhibition of TET1 or PARP1 can Rescue the Phenotypic Switching of MOVAS by Calcification

We further question whether the alteration of 5hmC modification caused the phenotypic switching of MOVAS with calcification. Therefore, we examined

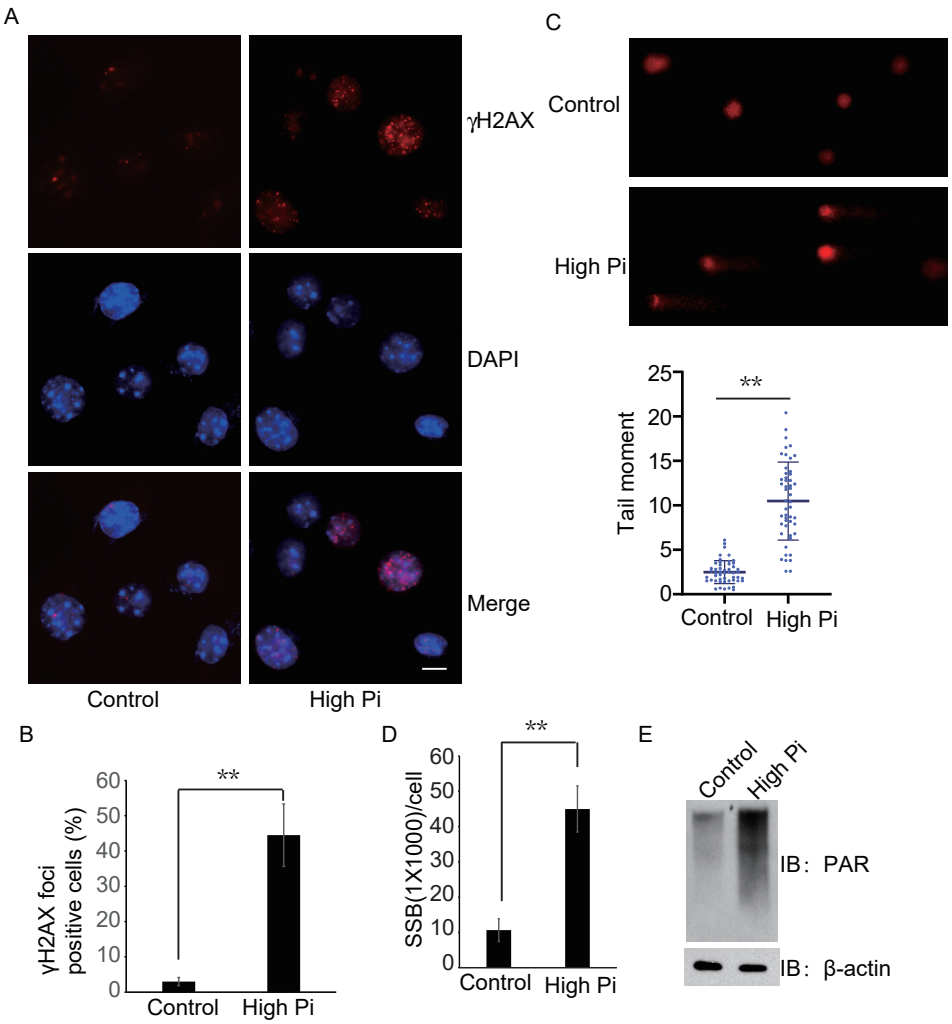

Fig. 3. High concentration of phosphate causes DNA damage in MOVAS

(A) γH2AX foci were examined by immunostaining to show the DSBs in MOVAS in either regular or calcification medium. Bar: 10 μm. (B) Percentage of γH2AX foci positive cells were summarized from immunostaining results. Fifty cells of each group were counted. The cell with γH2AX foci >5 was considered as positive. Three independent experiments were conducted. Data are presented as mean ± SD, $^{**}p<0.01$. (C) High concentration of phosphate significantly increased the SSBs in MOVAS. SSBs were examined by alkaline comet assay. Representative comet tails were shown. The tail moments were summarized from at least 50 cells, and 3 independent experiments were repeated. Data are presented as mean ± SD, $^{**}p<0.01$. (D) MOVAS cultured in regular or calcification medium were labeled with 3H-TdR. Then, the SSBs were analyzed as described in Materials and Methods. SSBs (mean ± SD, data from three independent experiments) were then summarized. Data are presented as mean ± SD, $^{**}p<0.01$. (E) Western blotting was conducted to detect the PAR level in MOVAS. High concentration of phosphate significantly increased the PAR level.

the effect of TET1 siRNAs and PARP1 inhibitor on α-SMA expression. The results indicated that both siTET1 and olaparib could rescue the α-SMA expression in MOVAS cultured with calcification medium **(Fig. 5A–C)**. To confirm the role of TET1 and PARP1 in phenotypic switching of MOVAS, we analyzed eight genes specifically expressed in either contractile SMCs or synthetic SMCs. Four genes, namely, MYH11, SM22α, SRF, and MYOCD, are specifically expressed in contractile SMCs. After phenotypic switching of SMCs by calcification, these genes decreased markedly **(Fig. 6A)**. By contrast, the other four genes, namely, ICAM1, CK8, KLF4, and LGALS3, increased during the transition from contractile SMCs to synthetic SMCs **(Fig. 6A)**. Consistent with the result of α-SMA, the alteration of all these genes medicated by calcification was attenuated by either olaparib or siTET1 but not mock siRNAs **(Fig. 6B–D)**.

Besides the decrease of SMC mark proteins, phenotypic switching of SMC is also characterized by high rate of cellular proliferation and increased pro-

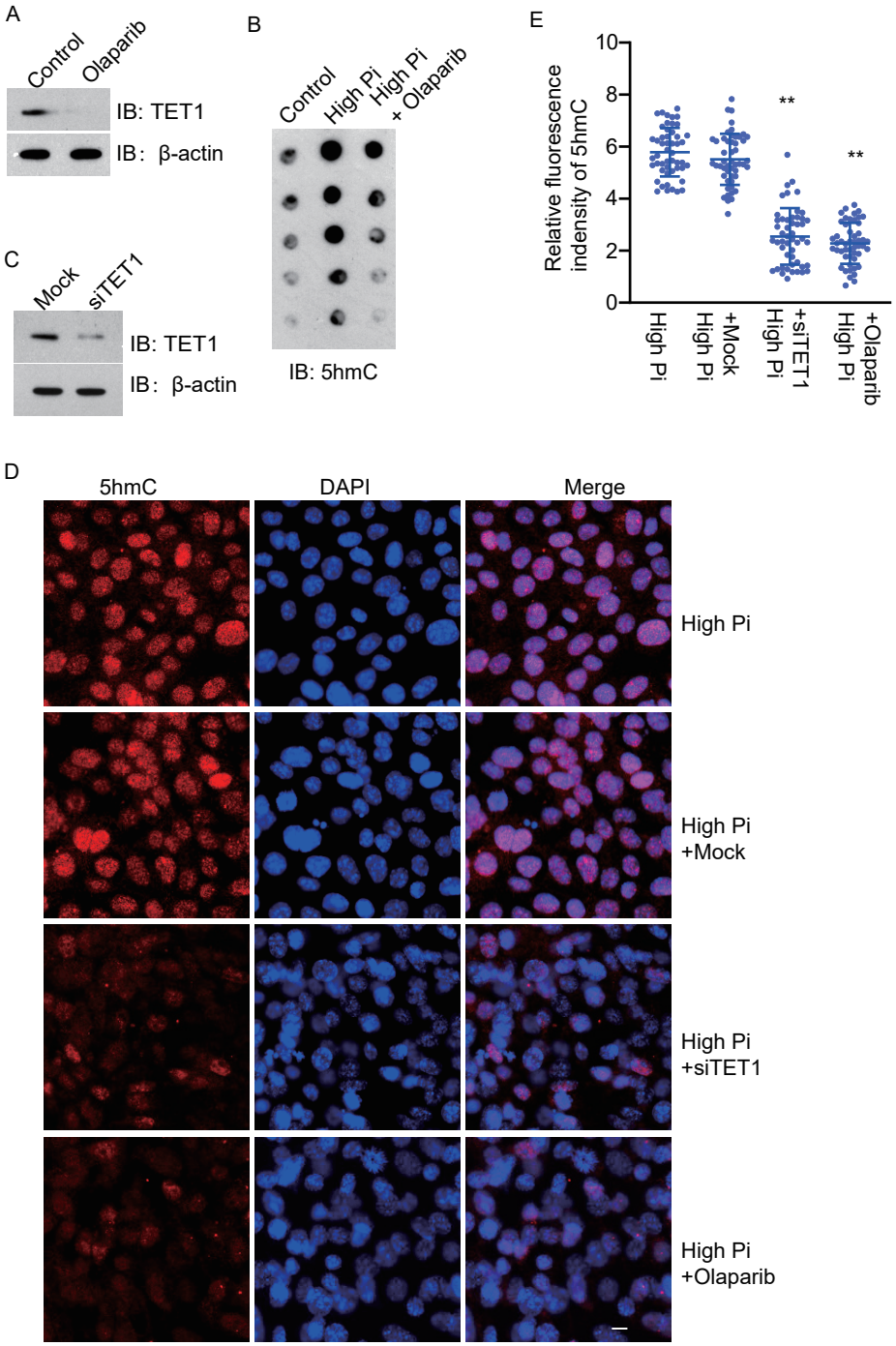

Fig. 4. Increase of 5hmC is mediated by PARylation in MOVAS with calcification medium culture

(A) High concentration of phosphate induced TET1 expression was regulated by PARylation. Olaparib significantly inhibited the expression of TET1 in MOVAS with high concentration of phosphate. (B) 5hmC level was examined by dot blotting. The increase of 5hmC level induced by calcification medium was markedly reversed by olaparib. (C) Western blotting was conducted to examine the effect of TET1 siRNAs. Mock siRNAs were used as control. (D) 5hmC level was further examined by immunofluorescence staining. Both siTET1 and olaparib could inhibit the 5hmC increase mediated by calcification. Bar: 10 μm. (E) Quantification of 5hmC level was summarized from the immunostaining results as shown in (D). Fifty cells in each group were analyzed by ImageJ. $^{**}p<0.01$.

duction of extracellular matrix[27]. To further confirm the effect of TET1 and PARP1 in phenotypic switching of MOVAS, we examined the proliferation of MOVAS in each group by conducting the immunostaining of Ki67, a proliferation marker, as described previously[28]. The results demonstrated that high-

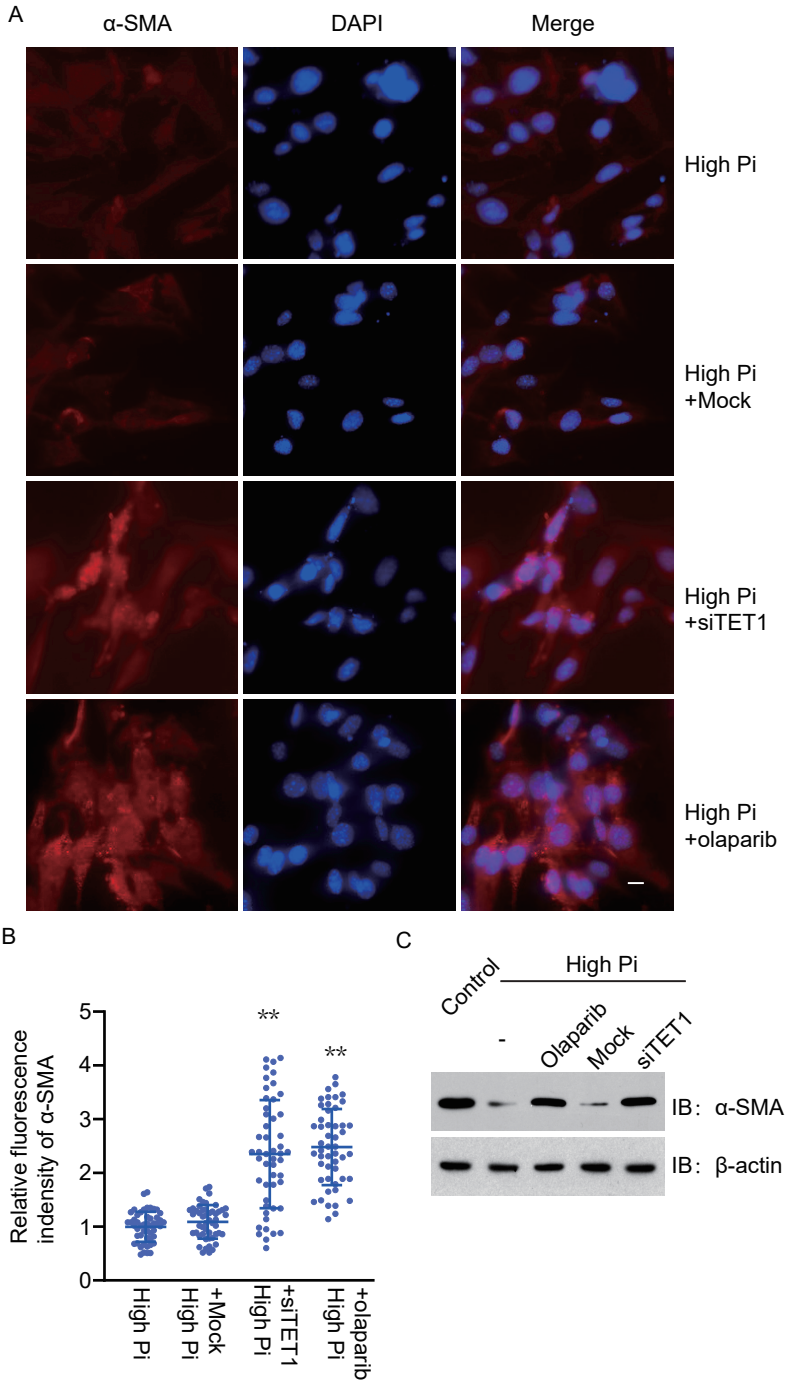

Fig. 5. Cell marker protein alteration of MOVAS is associated with PARylation-mediated 5hmC increase

(A) The expression of α-SMA was examined by immunostaining in MOVAS. Both siTET1 and olaparib could rescue the α-SMA decrease induced by high concentration of phosphate. Bar: 10 μm. (B) Quantification of α-SMA expression was summarized from the immunostaining results. Fifty cells in each group were analyzed by ImageJ. $^{**}p < 0.01$. (C) Western blotting was conducted to confirm the effect of siTET1 and olaparib on α-SMA expression under the high concentration of phosphate.

phosphate cultured cells were significantly more proliferative than control cells **(Fig. 6E–F)**. Consistent with the alteration of cell markers, both siTET1 and olaparib could reverse the increased proliferation induced by calcification medium in MOVAS **(Fig. 6E–F)**.

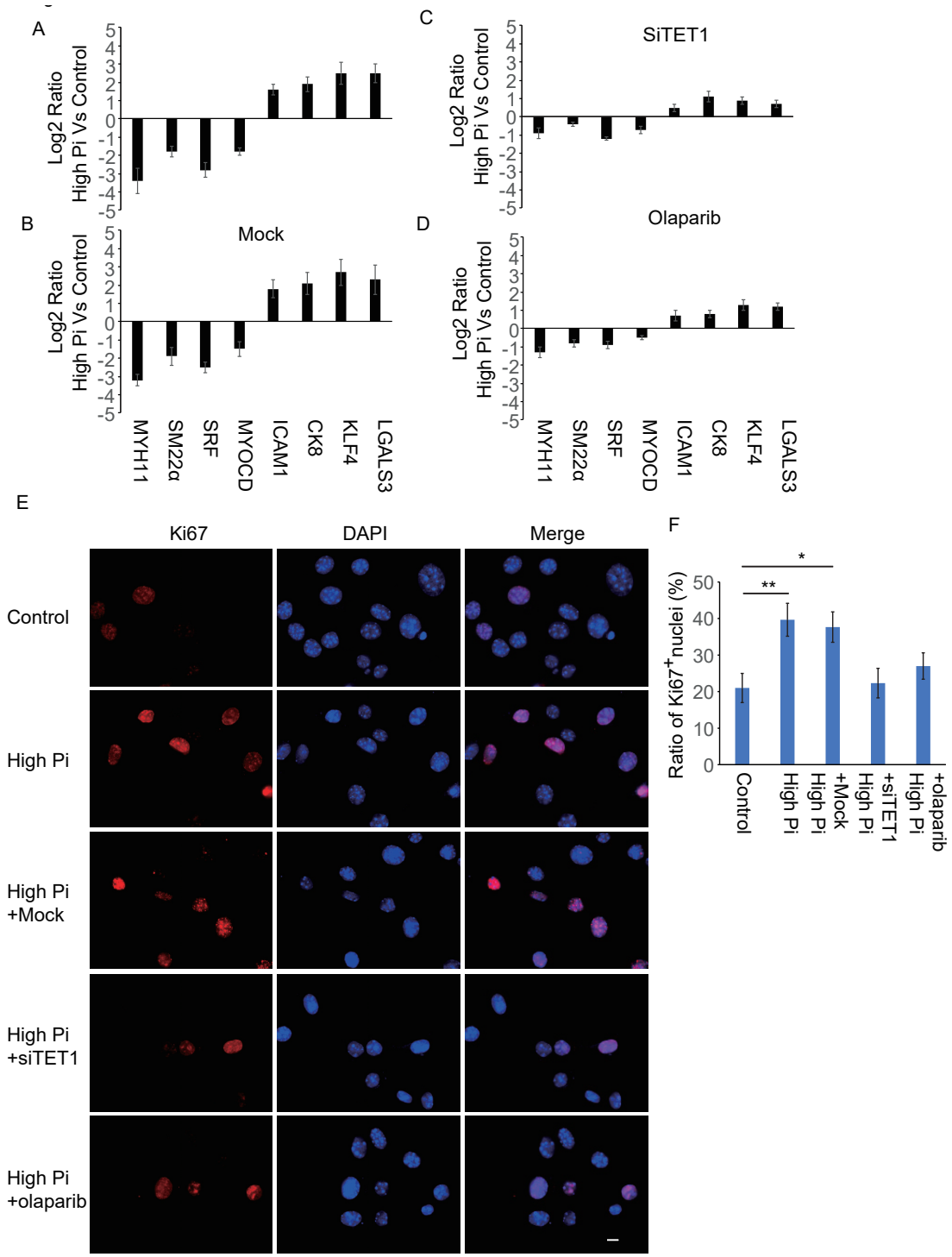

Fig. 6. PARylation-mediated 5hmC increase promotes phenotypic switching of MOVAS treated with high phosphate

(A–D) Eight genes specifically expressed in either contractile SMCs or synthetic SMCs were examined by qRT-PCR. During SMCs calcification, contractile SMCs specific genes decreased, whereas the synthetic SMCs genes increased (A). siTET1 and olaparib but not mock siRNA could reverse the above alteration of gene expression profile induced by calcification medium (B–D) shifted. Three independent experiments were conducted. Data are presented as mean ± SD. (E) Ki67 expression was examined by immunostaining to show the proliferation of MOVAS. Higher Ki67 expression has been shown in MOVAS cultured with calcification medium. siTET1 and olaparib, but not mock siRNA, could reverse Ki67 increase induced by calcification medium. Bar: 10 μm. (F) Quantification of Ki67 expression was summarized from the immunostaining results. Fifty cells in each group were counted to calculate the percentage of the Ki67 positive cells. $^{*}p < 0.1$, $^{**}p < 0.01$.

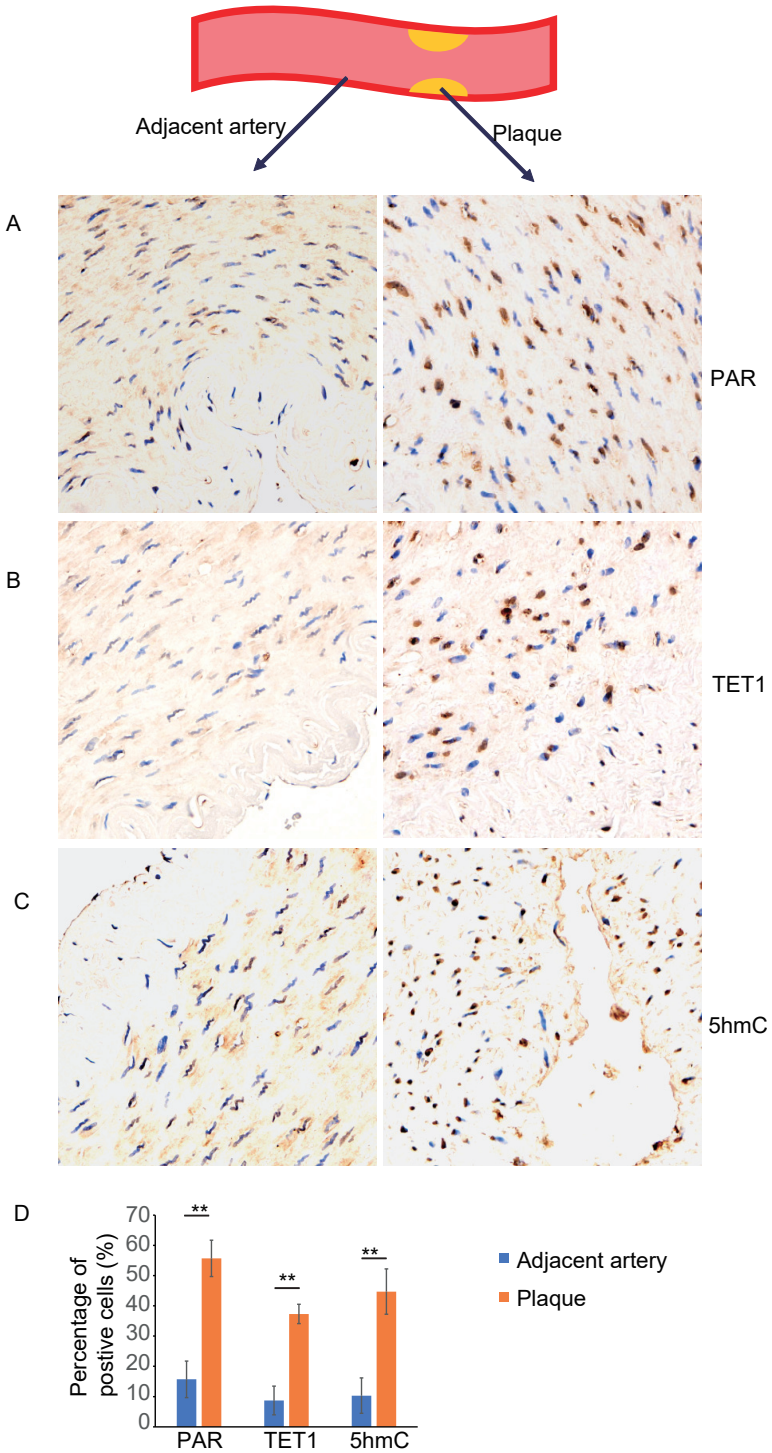

Fig. 7. PARP1-TET1 pathway is activated in the carotid atherosclerotic plaque

(A–C) Immunochemistry staining was conducted to examine expression of PAR, TET1, and 5hmC in carotid plaque as well as the adjacent artery tissue. Significant increase of PAR, TET1, and 5hmC positive cells was shown in carotid plaque compared with adjacent artery tissue. (D) Quantification of PAR, TET1, and 5hmC expression was summarized from the immunochemistry staining results. Fifty cells in each group were counted to calculate the percentage of the positive cells. $^{**}p < 0.01$.

PARP1-TET1 Pathway is Activated in the Carotid Atherosclerotic Plaque

Accelerated atherosclerotic calcification is believed to cause plaque burden in some pathological conditions, such as diabetes [29]. Therefore, to explore the potential application of the above *in vitro* findings, we collected the human carotid plaque from patients with atherosclerotic calcification in the carotid artery. Compared with the adjacent artery tissue, higher percentage of TET1, PAR, and 5hmC positive cells was shown in the carotid plaque. Since SMCs are the major source of plaque cells, our results indicated that PARP1 was also activated in SMCs in the atherosclerotic plaque[30], which is consistent with the results shown *in vitro* cell model **(Fig. 7A–D)**. However, to confirm that the increase of TET1 and 5hmC was caused by activated PARP1 in SMCs in the atherosclerotic plaque, further investigation in animal model is needed.

Discussion

In the present study, we demonstrated that oxidative stress causes DNA damage and activate PARP1 in the SMCs with calcification. Activated PARP1 further promotes the TET1 expression, resulting in the conversion of 5 mC to 5hmC. Alteration of DNA epigenetic modification is involved in the phenotypic switching of SMCs. Furthermore, our results indicated that inhibitors, such as siRNAs or small molecular drug, targeting either TET1 or PARP1 would rescue the phenotypic switching of SMCs with calcification. Hence, TET1 and PARP1 may act as the potential therapeutic target for atherosclerosis.

Accumulated evidences have shown the relationship between PARP1 and TET1. Ciccarone F. *et al.* reported that TET1 could interact with PARP1 and is the target of PARylation[31]. They further demonstrated that covalent PARylation can stimulate TET1 activity. Therefore, the increase of 5hmC levels in SMCs with calcification might be partially due to the PARylation modification in TET1 protein. However, based on our results **(Fig. 2E)**, the significant increase of TET1 expression may make the major contribution to 5hmC level in SMCs with calcification. A previous study indicated that enrichment of PAR on TET1 promoter encourages the TET1 transcription[32]. Although PARP1 itself can bind to TET1 promoter[32], it is more likely that PARylated transcription modulators are responsible for the TET1 transcription because PARP inhibitor, olaparib, can impair the TET1 transcription induced by calcification. To identify the PARylated transcriptors enriched on the TET1 promoter, further research is required.

As the first-step oxidized product of TET family proteins, 5hmC can be further oxidized to 5-formylcytosine and 5-carboxylcytosine[33]. Finally, the methyl group will be removed from the cytosine, so 5hmC is considered as the transient intermediate in DNA demethylation. However, 5hmC is also known as the stable epigenetic marker itself and associated with gene transcription[34]. But the relationship between 5hmC peaks and gene expression is complicated. High 5hmC enrichment is found in the gene bodies of active genes. By contrast, genes with low expression show an abundant 5hmC distribution at promoter regions[35]. We observed the increase of the genes related with synthetic phenotype and loss of gene markers of contractile phenotype in SMCs with calcification. This opposite effect on genes expression by calcification could be directly caused by 5hmC itself due to the different location of 5hmC enrichment or indirect regulating pathway; 5hmC ChIP-seq may be conducted in the future to elucidate the exact role of 5hmC in the gene profile change of SMCs phenotypic switching.

In conclusion, the present study demonstrated the relationship between two epigenetic regulation, PARylation and 5hmC, during SMCs phenotypic switching. Particularly, we found the increased PAR, TET1, and 5hmC shown in the carotid atherosclerotic plaque. Hence, it raises the possibility to target TET1 and PARP1 for atherosclerosis treatment as we know PARPs inhibitors have been used for the ovarian and breast cancer patients.

Acknowledgements

This research was supported by National Natural Science Foundation of China (81470587 to T.L and 81800483 to C.Z). For the remaining authors none were declared.

Conflicts of Interests

There are no conflicts of interest to declare.

References

1) Kramsch DM, Franzblau C and Hollander W: The protein and lipid composition of arterial elastin and its relationship to lipid accumulation in the atherosclerotic plaque. J Clin Invest, 1971; 50: 1666-1677
2) Badimon JJ, Fuster V, Chesebro JH and Badimon L: Coronary atherosclerosis. A multifactorial disease. Circulation, 1993; 87: II3-16
3) Bennett MR, Sinha S and Owens GK: Vascular Smooth Muscle Cells in Atherosclerosis. Circ Res, 2016; 118: 692-702

4) Gomez D and Owens GK: Smooth muscle cell phenotypic switching in atherosclerosis. Cardiovasc Res, 2012; 95: 156-164
5) Allahverdian S, Chaabane C, Boukais K, Francis GA and Bochaton-Piallat ML: Smooth muscle cell fate and plasticity in atherosclerosis. Cardiovasc Res, 2018; 114: 540-550
6) Jaenisch R and Bird A: Epigenetic regulation of gene expression: how the genome integrates intrinsic and environmental signals. Nat Genet, 2003; 33 Suppl: 245-254
7) He XW, Zhao Y, Shi YH, Zhao R, Liu YS, Hu Y, Zhuang MT, Wu YL, Li GF, Yin JW, Cui GH and Liu JR: DNA Methylation Analysis Identifies Differentially Methylated Sites Associated with Early-Onset Intracranial Atherosclerotic Stenosis. J Atheroscler Thromb, 2020; 27: 71-99
8) Khyzha N, Alizada A, Wilson MD and Fish JE: Epigenetics of Atherosclerosis: Emerging Mechanisms and Methods. Trends Mol Med, 2017; 23: 332-347
9) Turunen MP, Aavik E and Yla-Herttuala S: Epigenetics and atherosclerosis. Biochim Biophys Acta, 2009; 1790: 886-891
10) Erixon K and Ahnstrom G: Single-strand breaks in DNA during repair of UV-induced damage in normal human and xeroderma pigmentosum cells as determined by alkaline DNA unwinding and hydroxylapatite chromatography: effects of hydroxyurea, 5-fluorodeoxyuridine and 1-beta-D-arabinofuranosylcytosine on the kinetics of repair. Mutat Res, 1979; 59: 257-271
11) Wei R, Enaka M and Muragaki Y: Activation of KEAP1/NRF2/P62 signaling alleviates high phosphate-induced calcification of vascular smooth muscle cells by suppressing reactive oxygen species production. Sci Rep, 2019; 9: 10366
12) Zhuang J, Luan P, Li H, Wang K, Zhang P, Xu Y and Peng W: The Yin-Yang Dynamics of DNA Methylation Is the Key Regulator for Smooth Muscle Cell Phenotype Switch and Vascular Remodeling. Arterioscler Thromb Vasc Biol, 2017; 37: 84-97
13) Ito S, D'Alessio AC, Taranova OV, Hong K, Sowers LC and Zhang Y: Role of Tet proteins in 5 mC to 5hmC conversion, ES-cell self-renewal and inner cell mass specification. Nature, 2010; 466: 1129-1133
14) Tahiliani M, Koh KP, Shen Y, Pastor WA, Bandukwala H, Brudno Y, Agarwal S, Iyer LM, Liu DR, Aravind L and Rao A: Conversion of 5-methylcytosine to 5-hydroxymethylcytosine in mammalian DNA by MLL partner TET1. Science, 2009; 324: 930-935
15) Harrison D, Griendling KK, Landmesser U, Hornig B and Drexler H: Role of oxidative stress in atherosclerosis. Am J Cardiol, 2003; 91: 7A-11A
16) Singh U and Jialal I: Oxidative stress and atherosclerosis. Pathophysiology, 2006; 13: 129-142
17) Van Meter M, Simon M, Tombline G, May A, Morello TD, Hubbard BP, Bredbenner K, Park R, Sinclair DA, Bohr VA, Gorbunova V and Seluanov A: JNK Phosphorylates SIRT6 to Stimulate DNA Double-Strand Break Repair in Response to Oxidative Stress by Recruiting PARP1 to DNA Breaks. Cell Rep, 2016; 16: 2641-2650
18) Breslin C and Caldecott KW: DNA 3'-phosphatase activity is critical for rapid global rates of single-strand break repair following oxidative stress. Mol Cell Biol, 2009; 29: 4653-4662
19) Olive PL and Banath JP: The comet assay: a method to measure DNA damage in individual cells. Nat Protoc, 2006; 1: 23-29
20) Luo X and Kraus WL: On PAR with PARP: cellular stress signaling through poly (ADP-ribose) and PARP-1. Genes Dev, 2012; 26: 417-432
21) Caron MC, Sharma AK, O'Sullivan J, Myler LR, Ferreira MT, Rodrigue A, Coulombe Y, Ethier C, Gagne JP, Langelier MF, Pascal JM, Finkelstein IJ, Hendzel MJ, Poirier GG and Masson JY: Poly(ADP-ribose) polymerase-1 antagonizes DNA resection at double-strand breaks. Nat Commun, 2019; 10: 2954
22) Yang G, Liu C, Chen SH, Kassab MA, Hoff JD, Walter NG and Yu X: Super-resolution imaging identifies PARP1 and the Ku complex acting as DNA double-strand break sensors. Nucleic Acids Res, 2018; 46: 3446-3457
23) Chen JK, Lin WL, Chen Z and Liu HW: PARP-1-dependent recruitment of cold-inducible RNA-binding protein promotes double-strand break repair and genome stability. Proc Natl Acad Sci U S A, 2018; 115: E1759-E1768
24) Ray Chaudhuri A and Nussenzweig A: The multifaceted roles of PARP1 in DNA repair and chromatin remodelling. Nat Rev Mol Cell Biol, 2017; 18: 610-621
25) Jungmichel S, Rosenthal F, Altmeyer M, Lukas J, Hottiger MO and Nielsen ML: Proteome-wide identification of poly(ADP-Ribosyl)ation targets in different genotoxic stress responses. Mol Cell, 2013; 52: 272-285
26) Kaufman B, Shapira-Frommer R, Schmutzler RK, Audeh MW, Friedlander M, Balmana J, Mitchell G, Fried G, Stemmer SM, Hubert A, Rosengarten O, Steiner M, Loman N, Bowen K, Fielding A and Domchek SM: Olaparib monotherapy in patients with advanced cancer and a germline BRCA1/2 mutation. J Clin Oncol, 2015; 33: 244-250
27) Pidkovka NA, Cherepanova OA, Yoshida T, Alexander MR, Deaton RA, Thomas JA, Leitinger N and Owens GK: Oxidized phospholipids induce phenotypic switching of vascular smooth muscle cells in vivo and in vitro. Circ Res, 2007; 101: 792-801
28) Yang L, Gao L, Nickel T, Yang J, Zhou J, Gilbertsen A, Geng Z, Johnson C, Young B, Henke C, Gourley GR and Zhang J: Lactate Promotes Synthetic Phenotype in Vascular Smooth Muscle Cells. Circ Res, 2017; 121: 1251-1262
29) Li P, Wang Y, Liu X, Liu B, Wang ZY, Xie F, Qiao W, Liang ES, Lu QH and Zhang MX: Loss of PARP-1 attenuates diabetic arteriosclerotic calcification via Stat1/Runx2 axis. Cell Death Dis, 2020; 11: 22
30) Basatemur GL, Jorgensen HF, Clarke MCH, Bennett MR and Mallat Z: Vascular smooth muscle cells in atherosclerosis. Nat Rev Cardiol, 2019; 16: 727-744
31) Ciccarone F, Valentini E, Zampieri M and Caiafa P: 5 mC-hydroxylase activity is influenced by the PARylation of TET1 enzyme. Oncotarget, 2015; 6: 24333-24347
32) Li M, Tang Y, Li Q, Xiao M, Yang Y and Wang Y: Mono-ADP-ribosylation of H3R117 traps 5 mC hydroxylase TET1 to impair demethylation of tumor suppressor gene TFPI2. Oncogene, 2019; 38: 3488-3503
33) Ito S, Shen L, Dai Q, Wu SC, Collins LB, Swenberg JA, He C and Zhang Y: Tet proteins can convert 5-methylcy-

tosine to 5-formylcytosine and 5-carboxylcytosine. Science, 2011; 333: 1300-1303
34) Hahn MA, Szabo PE and Pfeifer GP: 5-Hydroxymethylcytosine: a stable or transient DNA modification? Genomics, 2014; 104: 314-323
35) Shi DQ, Ali I, Tang J and Yang WC: New Insights into 5hmC DNA Modification: Generation, Distribution and Function. Front Genet, 2017; 8: 100